Optimization of Redox Functionality Profiles of MoO_3–V_2O_5/ TiO_2 Composite Catalysts in Relation to Various Dispersion Patterns

Salah A. Hassan, Hamdi A. Hassan and Atef S. Darwish*

Department of Chemistry, Faculty of Science, Ain Shams University, Abbassia, Cairo, Egypt

Abstract: In the present study, a renewed approach was made to optimize the redox functionality of the well-known catalytic system MoO_3-V_2O_5/ TiO_2 (anatase) in relation to various dispersion patterns. Several types of composite catalysts were considered: xV/T (x of V_2O_5= 2-12 wt %), 6Mo-xV/T co-impregnates, yMo-8V/T co-impregnates (y of MoO_3 = 3-9 wt %), 6Mo-doped 8V/T (coat 1) and 8V-doped Mo/T (coat 2). The samples were characterized by adopting the XRD, FTIR, ESR, TEM, N_2 physisorption, high temperature H_2-chemisorption and high temperature O_2-chemisorptrion (HTOC), techniques. The redox reactivity was estimated in decomposition of H_2O_2 in highly concentrated solution, permitting the formation of several peroxo V intermediates. In xV/T system, the constancy of TON with loading indicated the involvement of single vanadia site, not sensitive to the surface dispersion, but rather depended on the nature of coordination of H_2O_2 molecules to VO_x species. For different co-impregnates of Mo and V, the added molybdena, increasing the Lewis acidity, seemed to undergo a competitive interaction with titania to form non-reducible surface compound, with increased density of surface VOx patches. This was confirmed from H_2-uptakes linked with highly stabilized V^{4+} species. The sample of coat 1had the same dispersion and reactivity patterns of the other members of co-impregnated series, with formation of non-reducible surface compound through Mo-O-V bridges. In coat 2 sample, the VOx species existed on the top surface of supported MoO_3/TiO_2 in a better dispersion state, with higher apparent density of surface patches, exhibiting comparable [A] and TON values to those of xV/T samples.

Keywords: MoO_3-V_2O_5 / TiO_2, Redox reactivity, Dispersion parameters, Peroxo complexes.

1. INTRODUCTION

Supported vanadium oxides are perhaps the most studied catalytic systems because of their industrial importance [1-6], especially when present as a monomolecular layer on the support surface. The support can enhance the thermal stability of dispersed oxide particles on the surface, contributing by several electronic effects [3-6]. The surface density of vanadia monolayer is known to be typically about twice that of many other metal oxides (*e.g.*, oxides of Mo, Cr, Re, etc.) [7], where the increased number of active sites minimizes the unwanted side reactions expected from the exposed support sites. The reactivity per site (TOF) for surface vanadia species in oxidation reactions is markedly larger than that of supported molybdena and chromia catalysts [7, 8].

Supported vanadia on anatase phase of titania could be distinguished as one of the most selective catalysts for many oxidation reactions, *e.g.*, of o-xylene [9, 10] and toluene [11, 12], for oxidative dehydrogenation of propane [13, 14] and for SCR of NO by NH_3 [15-17]. The highest specific activity of this type of catalysts could be only achieved when vanadia was present in monolayer or multilayer forms (but not crystalline V_2O_5) [18]. Their reactivity in oxidation and ammoxidation reactions was suggested to be a function of the vanadia–titania interaction, considered intermediate between V_2O_5–SiO_2 (weak) and V_2O_5–Al_2O_3 (strong), in view of the nature of surface-active layers formed [3, 18-21].

On the other hand, the addition of molybdena as a non-interacting promoter was found to develop the redox properties of vanadia, through changing the phase composition of surface layers and affecting the dispersion of monolayer VOx species on TiO_2, leading also to their higher reducibility characteristics [22-25]. In this respect, it was found for supported vanadia catalysts of loadings > 2.0 %, the reducibility was high and thus the redox characteristics were the main factors governing the catalytic reactivity, while for loadings < 0.5 %, the basic or acidic characteristics became the major factors controlling the catalytic reactivity [25]. The non-interacting additives are defined as metal oxides that preferentially coordinate with the oxide support rather than with the surface vanadia species under dehydrated conditions. They can only indirectly affect the molecular structure of the surface vanadia species via lateral interactions, influencing mainly the ratio of the polymerized to the isolated surface species, as on TiO_2 and Al_2O_3 but not on silica [6, 26, 27].

It is worth mentioning also, that the renewed interest in the peroxo-vanadium species, formed *in situ* by addition of H_2O_2 to NH_4VO_3 in acidic aqueous solutions

*Address correspondence to this author at the chemistry department, faculty of science, Ain-Shams University, Cairo 11566, Egypt; Tel: +202 24831836; Fax: +202 24831836; E-mail: atef_mouharam@sci.asu.edu.eg

E-ISSN: 2408-9834/19

has been stimulated by their biochemical importance [28-31], recorded for instance as potential insulin mimics with an ability to inhibit the phospho-proteins activity. This could attract many authors to re-examine the reaction from different angles and to reuse it in the oxidation of aromatic hydrocarbons under ecologically acceptable reaction conditions [*e.g.*, 31-35].

The present work was undertaken to study the effect of addition of MoO_3, in different ratios and in different sequences, on the various structural, textural and dispersion characteristics of the V_2O_5/TiO_2 (anatase) catalytic system, of different loadings approaching the monolayer formation. The redox reactivity was discussed in view of the peroxo-intermediates formed during the reaction with H_2O_2 in highly acidic conditions. This should provide some additional knowledge for several SCR and oxidation applications.

2. EXPERIMENTAL

2.1. Catalyst Preparation

The xV_2O_5/TiO_2 samples with vanadia loading (x) ranged between 2 and 12 wt% were prepared by impregnating TiO_2 (anatase, PROLABO) with appropriate concentration of ammonium meta-vanadate (NH_4VO_3, BDH) in aqueous solution, using oxalic acid as complexing agent. The mixture was stirred for 12 h for homogenization and dried gradually at 110^o C overnight. The product was calcined in atmospheric air at 450^o C for 4 h for complete decomposition to V_2O_5, avoiding the transformation of anatase to rutile and formation of V–Ti oxides [11]. Two series of co-impregnates were prepared, namely, of ($8V_2O_5$-$yMoO_3/TiO_2$) containing 8 wt% vanadia and y MoO_3 = 3 – 9 wt% and those of (xV_2O_5-$6MoO_3$) containing 6 wt% MoO_3 and x V_2O_5 = 3 and 5 wt%. They were prepared via co-impregnation of TiO_2 support with binary aqueous mixtures of NH_4VO_3 complexed with oxalic acid and $(NH_4)_6Mo_7O_{24}.4H_2O$ complexed with citric acid of required concentrations. For extended study of the doping effect of either MoO_3 or V_2O_5, two additional samples containing 8 wt % V_2O_5 and 6 wt% MoO_3 were prepared. In the first one, the already supported 8 wt% V_2O_5/TiO_2 catalyst was impregnated with ammonium heptamolybdate solution of the appropriate concentration (MoO_3-doped V_2O_5/TiO_2, coat 1). In the second, the already supported 6 wt% MoO_3/TiO_2 catalyst was impregnated with ammonium meta-vanadate solution of the appropriate concentration (V_2O_5-doped MoO_3/TiO_2, coat 2). The remained procedure was applied as mentioned above.

2.2. Catalyst Characterization

The solid materials were characterized by powder X-ray diffraction recorded on a Brucker D8 advance X-ray diffractogram with Cu Kα radiation (λ = 1.5418 Å). FT-IR spectra were measured using AT1 Mattson model Genesis Series (USA) infrared spectrophotometer. The KBr technique was carried out approximately in a quantitative manner, as the weight of the sample and that of KBr were kept constant. For studying the TEM images, a ZEISS EM-10 transmission electron microscope equipped with a 60 KV source was used. The sample was dispersed in water and deposited on a carbon film supported on a copper grid. The ESR spectra were recorded on a Brucker ELEX-SYS 5000 spectrometer operated at X–band frequency, with the ER–4131 VT variable temperature accessory, at room temperature and at liquid nitrogen temperature. N_2 adsorption-desorption isotherms at -196^{o}C were measured using a NOVA 3200 apparatus, USA. The samples were pretreated by out gassing under vacuum at 300^o C for 3 h. Surface areas (S_{BET}) were calculated from multi-point at P/Po range, 0.05 – 0.30, and pore size distributions were estimated by using the BJH method.

As a relevant approach, the high temperature oxygen chemisorption (HTOC) isotherms at 365^o C, measured in a conventional volumetric micro system [36], were used for estimating the dispersion parameters of supported VO_x species. A standard pretreatment of the samples involved reduction *in situ* at 520^o C for 4 h, [3], followed by out-gassing at the same temperature for 2 h, at p ~10^{-5} torr (1 torr = 1.33 x 10^2 Pa). From the evaluated O_2 uptakes, after correction for titania support, the degree of dispersion of supported V_2O_5, (D = O/V) was calculated as the ratio of number of oxygen atoms chemisorbed (equivalent to number of exposed V atoms, N_V): total number of V atoms in the sample. Also, the active site density, (ASD), was expressed as the number of exposed V atoms per nm^2 of TiO_2 surface area. The metallic surface area of exposed vanadia (S_V) per gram active phase was calculated as the number of exposed V_2O_5 molecules multiplied by 2 σ_V, (σ_V, the area occupied per $VO_{2.5}$ unit = 0.103 nm^2 [37]). The average particle size (a_e, nm) of V_2O_5, was determined based to

first approximation on the cubic crystallite model [36], by the equation: $a_e = (5 \times 10^4) / (S'_V \times \rho_V)$, ρ_V is the density of V_2O_5 taken as 3.36 g ml^{-1} [38]. Also, a patch model was suggested, following similar lines of discussion described elsewhere [27, 37], taking into account the orthorhombic crystallite form with a volume of unit cell (c) = 0.0902 nm^3 [38]. A rough estimate of number of surface patches of supported V_2O_5 species per gram catalyst (N_V^*) was made by the equation, $N_V^* = N_V . c / d_V^3$, (where, d_V^3/c is the number of orthorhombic unit cells per particle, N_{uc}, considered approximately as the patch size). The relative density of V surface patches (α^*_V) could also be considered as patch size/S_{TiO2}.

2.3. Redox Reactivity Estimation

The redox activities of the various samples were evaluated in the decomposition of concentrated H_2O_2 (30% volume), in highly acidic conditions (pH = 2.0), permitting the formation of several intermediate peroxo-complexes. From the measurements of volume of O_2 evolved, at different conditions, both the activity parameter (A) and the turnover number (TON) were estimated per active vanadia site (N_V) [36, 37] and were discussed in view of the peroxo complexes formed and in correlation with the different dispersion regimes.

3. RESULTS AND DISCUSSION

3.1. Structural Characteristics of Various Samples Under Study

From the XRD patterns depicted in Figure **1** for various V/T samples, it is clearly shown that no characteristic peaks of crystalline V_2O_5 phase could be detected below 8 wt % vanadia. Only above this loading, some small clusters of V_2O_5 crystallites could be revealed (of d spacings: 4.37, 3.41 and 2.88 Å), referred most probably to the crystallized orthorhombic V_2O_5 of Scherbinite type [39]. This could indicate that the monolayer formation is starting near this loading, compared with 7.4 wt% in many other works [*e.g.*, 7, 8, 37]. Below this ratio, vanadia tended to exist in some highly dispersed nature. Addition of MoO_3, in any ratio, in co-impregnation with 8 wt % V/T could lead to marked diminution of characteristic vanadia peaks, which might be related to the strong interaction of MoO_3 with TiO_2, influencing the dispersion nature of V_2O_5 particles on the surface. No characteristic bands of new interaction phases could be detected.

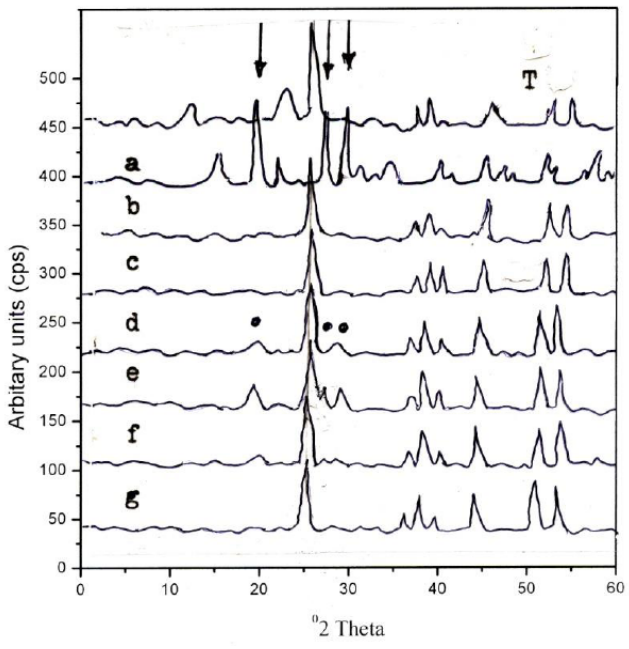

Figure 1: XRD patterns of bulk V_2O_5 (**a**), x V/T samples; x = 2 (**b**), x = 5 (**c**), x = 8 (**d**), x = 20 (**e**), 6Mo – 8V/T (**f**) and 9Mo – 8V/T (co-impregnated) sample (**g**).

The FTIR analysis revealed that for the sample 2V/T (Figure **2-a**), neither the band at 1020 cm^{-1} assigned for bulk V_2O_5 crystallites nor that one at 980 cm^{-1} assigned for the amorphous monolayered VO_x species could be observed, due to its high dispersion nature. For higher vanadia loadings, viz., 5V/T and 8V/T samples the weak band at ~1020 cm^{-1} indicated the appearance of crystallite clusters of surface V_2O_5. Upon addition of 6 wt % Mo to the 8V/T sample, in different sequences (Figure **2-b**), the band at 1020 cm^{-1} disappeared and instead two weak bands appeared in the region 970 – 983 cm^{-1}, corresponding to monolayered amorphous VO_x species or polymeric VO_4 units (both with ν(V=O) stretching modes, [6, 40]. The effect was much pronounced in the sample of coat 1 ($6MoO_3$–doped 8V/T). For evidence, using higher ratio of MoO_3, namely 9 wt% in the sample 9Mo–doped 8V/T, (Figure **2-c** (i)), two clear bands appeared, at 987 cm^{-1} and at 894 cm^{-1}, both of weakened V=O bond with modified strengths [40] (for Mo=O in hydrated form, the bands in 960 – 930 cm^{-1} region were reported [23, 40]). This could suggest that the added molybdena has weakened the interaction of VO_x crystallites with TiO_2 surface, leading to dissociation of part of them into amorphous mono-layered species (*i.e.*, amorphization). Less ratio of MoO_3 (3.0 wt %) in all preparations (2-c (ii), (iii) & (iv)) could not affect the band at 1020 cm^{-1} due to weaker competitive role of Mo.

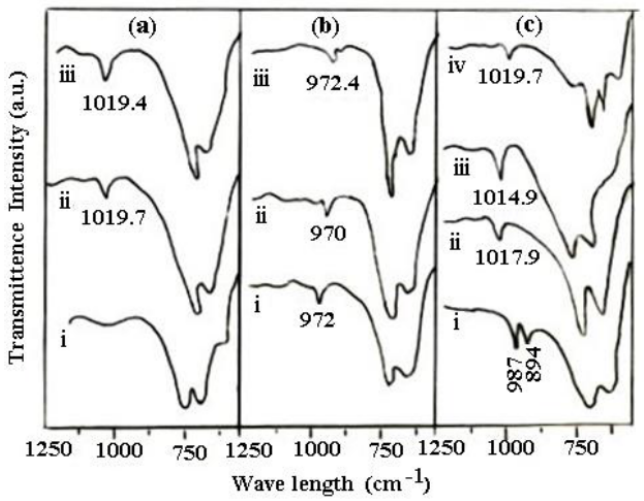

Figure 2: FTIR spectra of: **(a)** x V/T samples; [x = 2 (i), x = 5 (ii), x = 8 (iii)], **(b)** 6Mo–doped 8V/T (coat 1) (i), 8V–doped 6Mo /T (coat 2) (ii), 6Mo–8V/T co-impregnates (iii) and **(c)** 9Mo–doped 8V/T (coat 1) (i), 3Mo–doped 8V/T (coat 1) (ii), 8V– doped 3Mo /T [coat 2] (iii), 3Mo–8V/T co-impregnates (iv).

The obtained ESR spectra at 77 K for pure titania support, bulk V_2O_5, supported 8V/T catalyst sample and 6Mo-8V/T co-impregnated sample are depicted in Figure **3**. Two weak signals were occurred for pure titania; the sharpest was assigned at g=1.942 most probably due to Ti^{3+} species produced through the initial thermal treatment [41]. For bulk V_2O_5, a sharp signal (of Lorentzian shape) with slight hyperfine splitting was occurred at g = 1.97, of magnetically interacting V^{4+} species in a slightly reduced V_2O_5 in the bulk phase [42]. For supported 8V/T catalyst sample, approaching the theoretical monolayer formation of vanadia, the obtained spectrum suggested the existence of the same species as in the bulk V_2O_5; the non-stoichiometric $V_2O_{5-\delta}$ crystalline particles seemed to be prevailing on the surface [43]. As spontaneous reduction of V^{5+} to V^{4+} was reported to occur at the V_2O_5–TiO_2 interface during the calcination at t > 450° C [21], mixed V^{4+}-O-V^{5+} bridges could be proposed to take place through exchange interactions between adjacent V^{4+} species [44, 45]. Upon addition of MoO_3, in the 6 Mo-8 V/T co-impregnated sample, the obtained more sharp ESR signal at g=1.97, without any splitting, may be interpreted in view of the superposition of strong Mo^{5+} signal to the V^{4+} features of the 8V/T sample, suggesting several electronic interactions, involving V^{V}, V^{IV}, Mo^{VI} and Mo^{V}, through O-bridging [45, 46].

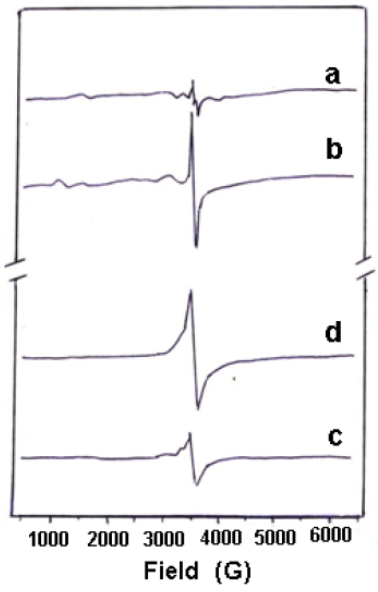

Figure 3: ESR spectra of: (**a**) pure titania and (**b**) bulk V_2O_5, (**c**) 8V/T and (**d**) 6Mo – 8V/T [co-impregnates].

3.2. Textural and Morphological Characteristics

The obtained adsorption – desorption isotherms of N_2 over the surface of pure TiO_2 (anatase) support, bulk V_2O_5 and various supported V_2O_5, MoO_3, and MoO_3 – V_2O_5 on TiO_2 samples were completely reversible, of type II according to IUPAC classification. All the isotherms reflected the main adsorption behavior of the titania support. The derived surface parameters, are summarized in Table **1**, including specific surface areas (S_{BET}, m^2 g^{-1}), pore volumes (V_p, ml g^{-1}) estimated from the saturation values of the isotherms and average pore radii (r_p^{cp}, nm) assuming cylindrical pore model (cp). From the results obtained, a marked decrease could be noticed upon loading vanadia on TiO_2 surface. Above ca. 3 wt% V_2O_5, of average surface density 3.5V/ nm^2, the surface area and pore dimensions became somehow less sensitive to V loading [47]. In all cases, mesopores with an average radius of ca. 2–3 nm seemed predominating. Upon addition of different ratios of MoO_3, in co-impregnation with 8 wt % V_2O_5, some slight increase in pore volume (to ca. 0.15 ml g^{-1}), pore radius (to ca. 4 nm), compared to the reference 8 V/T sample, reflected the effect of the additive (especially 6 wt%) on the nature of vanadium–titania interaction (V–O–Ti bridges) [48]. For more evidence, the samples containing the same 6 Mo % in co-impregnation with V/T of different vanadia contents, viz., 3, 5, and 8 wt %, showed a gradual increase in surface parameters with the increase in vanadia loading. Specifically, that sample prepared by coat 1 method, (6 wt% MoO_3 – doped 8V/T), could be distinguished by its highest surface

Table 1: Textural, Surface Dispersion and Redox Activity Parameters of Various Supported V_2O_5/TiO_2 and MoO3 - V_2O_5/TiO_2 Catalytic Systems

Catalyst Sample	Surface Parameters			Dispersion Parameters					Activity Parameters		
	S_{BET} $m^2\ g^{-1}$	V_P $mL\ g^{-1}$	r_h Nm	D (O/V)	ASD Vnm^{-2}	S_V (x 10^{20}) $m^2\ g_{V2O5}^{-1}$	α^*_V	a_e (nm)	k min^{-1}	[A] molec $_{H2O2}$ $min^{-1}.\ g_{V2O5}^{-1}$	TON
T	105.4	0.138	2.6								
x V/T x (wt% V_2O_5) :											
2	72.1	0.100	2.8	0.53	1.0	360	0.03	4.1	0.021	126	5
3	56.6	0.069	2.4	0.45	1.6	304	0.46	4.9	0.023	138	5
5	59.4	0.066	2.2	0.39	2.2	263	0.62	5.6	0.053	204	5
8	57.5	0.081	2.8	0.35	3.2	239	0.83	6.2	0.126	306	5
12	-----	-----	-----	-----	------	-----	----	----	0.147	----	---
V_2O_5	143.9	0.154	2.1	-----	------	------	----	-----	-----	-----	----
8V–yMo/T, y (wt% MoO_3) co-impregnates											
3.0	70.5	0.100	2.9	0.32	2.2	203	0.66	7.3	0.120	288	6
4.5	67.1	0.145	4.3	0.28	2.0	201	0.69	7.8	0.112	318	7
6.0	71.1	0.113	2.8	0.16	1.3	178	0.70	9.8	0.111	335	8
7.5	60.4	0.101	3.4	0.12	1.0	157	0.73	11.3	0.129	358	8
9.0	67.3	0.860	2.5	0.04	0.8	96	0.98	15.5	0.131	366	16
xV–6Mo/T, x(wt% V_2O_5) co-impregnates											
3	59.4	0.079	2.6	0.83	2.8	563	0.58	2.6	0.038	222	5
5	60.6	0.093	3.1	0.10	0.6	70	0.17	21.3	0.050	280	19
8V–6Mo/T											
Coat 1	129.9	0.128	2.0	0.29	1.3	195	0.42	7.6	0.104	318	7
Coat 2	78.0	0.095	2.4	0.42	1.3	293	0.70	5.1	0.160	336	5

area, even higher than that of pure titania, while pore dimensions remained close to that of titania. This could confirm the effect of added molybdena on the dispersion state of supported vanadia via controlling the aggregation of VO_x species on the surface with limited penetration in support pore system.

The morphology of different samples under study was investigated as represented in Figure **4**. The image (a) of pure titania support, treated at 450° C for 4 h, revealed microcrystalline particles of different sizes ranging from <50 nm to several hundreds of nm, characteristic of agglomerates forming a porous structure with voids of different shapes. In the image (b) of 8V/T, vanadia seemed as dispersed particles fused together, approaching the monolayer formation. Part of these particles of sizes < 5 nm tends to penetrate in titania voids (elements 1, 2 & 3), while larger agglomerates appear in layers over the support surface (elements 4, 5 & 6). The image (c) of co-impregnated 6 Mo–8V/T represented one phase distributed entirely on titania particles, where molybdena seemed preferentially covering the support surface in larger sizes (*e.g.*, 1, 2 & 3). Some amorphized phase could be indicated as an interaction product between Mo and V, while the titania microstructure was retained. In image (d) of coat 1 (6 Mo-doped 8V/T), Mo addition led to spreading of vanadia species in isolated patches on the surface. However, in image (e) for coat 2 (8V-doped 6Mo/T), coalescence of the interaction product was clearly shown, in terms of competitive linkages with the surface, likely with some mobility of different phases on the surface.

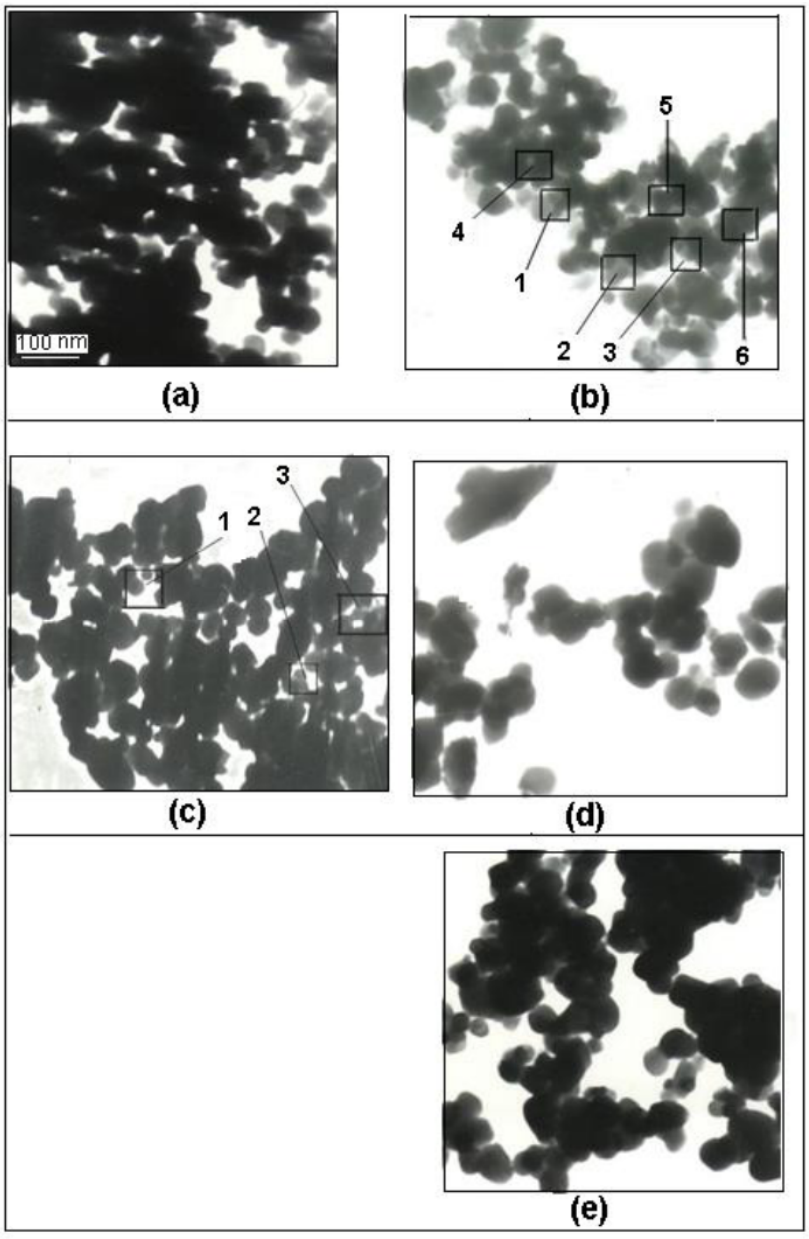

Figure 4: Transmission electron micrographs of: (**a**) pure titania, (**b**) 8V/T sample, (**c**) 6Mo − 8V/T co-impregnate (**d**) 6Mo−doped 8V/T [coat 1] and (**e**) 8V−doped 6Mo/T [coat 2].

3.3. Surface Dispersion Profiles of the Supported Oxides

The obtained HTOC isotherms (at 365° C) are depicted in Figure **5** (**a**) for x V/T samples and in Figure **5**(**b**, **c**) for different x V – y Mo samples, pretreated through high temperature reduction for 4h. From the variation of stationary values of O_2 uptakes (μmol O_2 g^{-1} catalyst) with V loading (%), monolayer coverage of TiO_2 surface seemed to be approached. Moreover, from the slope of this variation plot at low loadings estimated to be = 0.5, it could be assumed that one O atom corresponds to two V atoms. This value could also be accepted as representing the HTOC stoichiometry on the reduced vanadia samples, according to, $V_2O_5 + H_2 = V_2O_4 \square + H_2O$ and $V_2O_4 \square + O = V_2O_5$ (where, □ denotes a coordinatively unsaturated site, CUS, upon which oxygen chemisorption occurs). It seemed thus, that by dissociative chemisorption of O_2, the partially reduced V particles form dimeric VO_x species, rather than monomeric ones, most likely in one-dimensional clusters. The calculated degrees of dispersion (D) of supported V_2O_5 (*i.e.*, O/V), in view of the proposed stoichiometry, are included in Table **1**, showing a gradual decrease with vanadia loading. The active

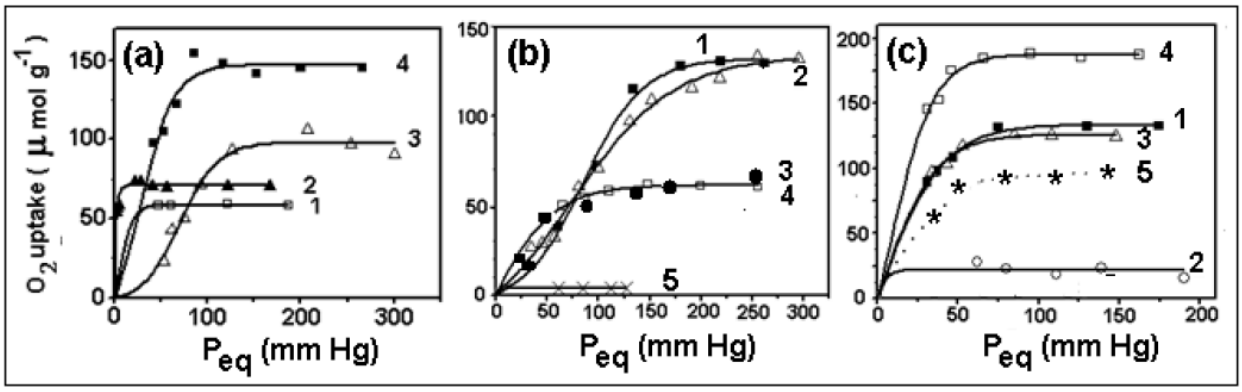

Figure 5: HTOC isotherms on **(a)** xV/T: [x (wt %) =2 (1), x= 3 (2), x= 5 (3), x= 8 (4)]; **(b)** yMo–8V/T co-impregnates:[y (wt%) = 3 (1), y= 4.5 (2), y= 6.0 (3), y= 7.5 (4), y= 9.0 (5); 3 (1), 4.5 (2), 6.0(3), 7.5(4), 9.0(5); **(c)** 6Mo–x V co-impregnates: x= 3 (1), x= 5 (2), 6Mo–doped 8V/T (coat 1) (3); 8V–doped 6Mo/T (coat 2) (4) and 6Mo/T (5).

surface density (ASD), taken as the number of exposed vanadium atoms per unit surface area of the reduced catalyst sample, increased with % V loading and consequently the metallic surface area of surface dispersed vanadia (S_V) decreased, while the average VOx particle size (a_e), based to first approximation on the cubic model, gradually increased. All these results indicated the continuous aggregation of surface VOx species with increasing the V% loading. On the hand, based on the *patch* approach corrected to the orthorhombic crystallite form of vanadia [27, 37], the apparent density of surface patches (α^*_V) showed a continuous increase with the increase of % loading (Table **1**). This could confirm the obvious increase in the number of CUS responsible for O_2 chemisorption, up to the monolayer level, existed most probably as surface patches with increasing sizes (with structures ranging from strongly interacted isolated V^{IV} species to oligomers, or clusters weakly interacted with TiO_2 [45-48].

For the different samples prepared by co-impregnation of 8 wt % V_2O_5 with different ratios of MoO_3 ranging from 3.0 to 9.0 wt%, it is clear from Table **1** that, the addition of molybdena has led to a gradual decrease in degree of dispersion of surface vanadia (D, ASD and S_V). Consequently, the average particle size of VOx species in view of cubic model (a_e) increased, with a less effect on the apparent density of surface patches (α^*_V), the size of which was corrected for the orthorhombic crystallite form. The obtained results could suggest the preferential interaction of molybdena with titania surface, leading the particles of vanadia to be aggregated in larger particles, with somewhat increased size of surface patches. Another possibility could be assumed for these systems, namely the interaction of molybdena with vanadia to form a surface compound, difficult to be reduced. For instance, the study of H_2 chemisorption uptakes, of prime interest for the high temperature reduction pre-treatments [36, 49]), are depicted in Figure **6** for V_2O_5, 6 Mo−doped 8 V/T (coat 1) and 8V-doped 6Mo/T (coat 2). Extremely higher uptakes exhibiting most probably H-spillover [36], could be revealed, in contrast to the 8V/T and 6Mo/T. This phenomenon appeared to be linked with formation of highly stabilized reduced species (*e.g.*, V^{3+} and V^{4+} species) resistant to further reduction and re-oxidation processes [24]

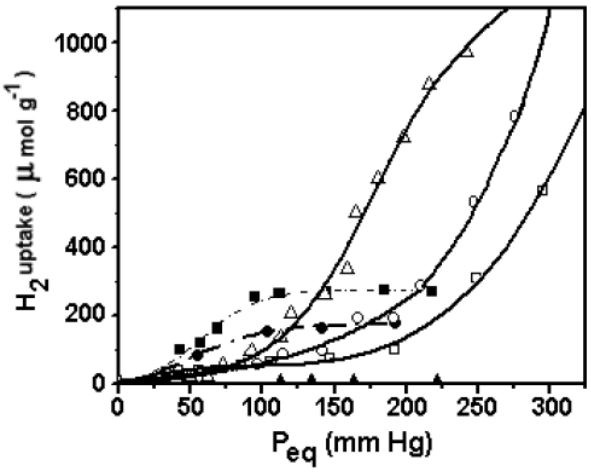

Figure 6: H_2 uptakes at 520°C on: bulk V_2O_5 (Δ), 6 Mo−doped 8 V/T (coat 1) (o), 6 Mo–8 V/T co–impregnate (□), 8V/T (■), 8 V–doped 6 Mo/T (coat 2) (●) and 6 Mo/T (▲).

On the other hand, the sample containing 9.0 wt% MoO_3 showed markedly larger patches density, most probably growing three dimensionally, with an obvious decrease in vanadia dispersion (Figure **5**, **b**, **5**). However, for the co-impregnated sample of 6 Mo–3 V/T, surface vanadia appeared to exist as separate

monomeric species where the added molybdena, by competitive linkage with titania, rendered vanadia particles more dispersed on the surface. By inhibiting the re-aggregation process, more number of much smaller patches of VO_x species could be observed (*i.e.*, amorphization-like mechanism). Again, the dispersion decreased considerably when vanadia loading rose to 5 wt %, in the same manner as the other samples approaching the monolayer formation. In the sample of coat 1, (6 Mo–doped 8V/T), the added molybdena after vanadia impregnation in almost monolayer, had most likely more chance to interact with VOx species to form the non-reducible surface compound (confirmed again by higher H_2 uptakes in Figure **7**). The decrease in degree of dispersion took place via redistribution of surface VO_x species, with less density of surface patches. The stationary amounts of O_2-chemisorbed (125 μ mol O_2), had a close trend to that of 6 Mo/T sample (~100 μ mol O_2). In the sample of coat 2, (8 V–doped 6 Mo/T), the added vanadia seemed to locate on the top surface of interacted Mo in relatively better dispersion state with less particle sizes than in the 8V/T sample. These top species existed in higher density of surface patches, probably in a different structure, easily reduced and easily re-oxidized [21].

3.3. Redox Activity of the Investigated Samples

The different peroxo-complexes, known to be formed through the reaction of H_2O_2 with vanadium species to produce dioxygen species via self-decomposition, are shown in Scheme **1** [32]. All these species can be used for several chemical and biochemical oxidation systems.

In view of this scheme, the red cationic monoperoxo $[VO(O_2)]^+$ species and anionic diperoxo complexe $[VO(O_2)]^-$ were reported to be dominant at pHs < 2 and in 3–5 range, respectively. The anionic diperoxo complex is converted into the anionic triperoxo species $[V(O_2)_3]^-$ by further addition of H_2O_2, which is assumed an important active intermediate in several oxidation processes [33]. In highly concentrated solution of H_2O_2, as in our study, the triperoxo intermediate (X_1 in Scheme **1**) of increased concentration is transformed into the superior oxidant (X_2), involving a two-electron transfer between two coordinated peroxo groups in the rate limiting stage [33]. This active super oxidant intermediate undergoes a self-decomposition into dioxygen and inactive V^V peroxo species (viz., V^V= O and V^V– O^-), that may in turn form diperoxo species again in a fast irreversible reaction or may react with H_2O_2 in a reversible redox step to form green vanadyl $(VO)^{2+}$.

Considering the limiting rate of transformation of X_1 to X_2 (Scheme **1**), the redox activity of various catalyst samples under study, could be expressed in terms of the first-order rate constant (k, min^{-1}) of H_2O_2 decomposition reaction at 30° C in strong acidic conditions (pH=2), permitting the formation of different peroxo-complexes at different stages. The results are represented in Figure **7** (**a** & **b**) as a function of wt% vanadia loading. Linear relationships were evident for the different catalyst systems studied, the slope of which appeared to be dependent on the catalyst characteristics.

For x V/T samples, almost similar trend is shown in Table **1** for k (min^{-1}) and the activity parameter [A], denoting the number of H_2O_2 molecules consumed per

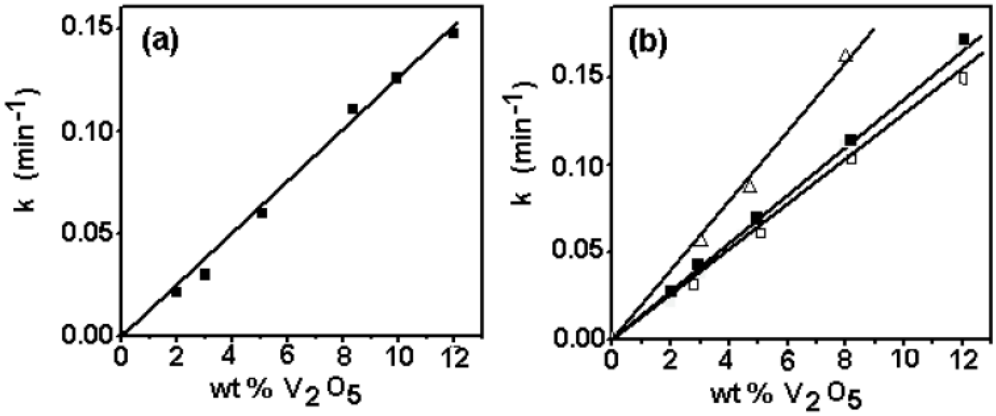

Figure 7: The redox activity, $k_{1\ H2O2}$ (min^{-1})], as a function of wt % V_2O_5 in: (a) x V/T catalyst samples of different loadings, and (b) 6Mo – x V/T samples prepared by: co-impregnation (■), 6Mo-doping supported V/T (coat 1) (□) and V-doping supported 6Mo/T (coat 2) (Δ).

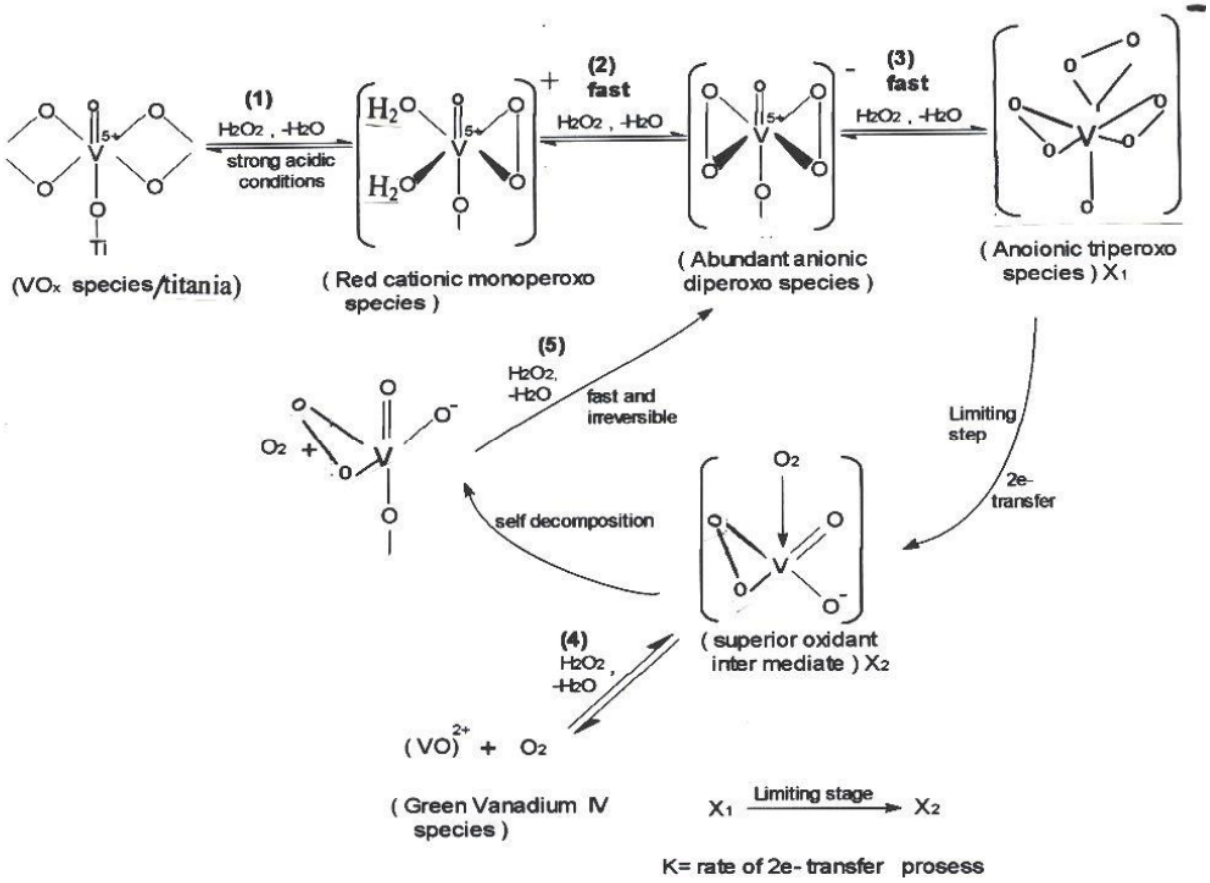

Scheme 1: Different peroxo V intermediates.

unit time per gram supported V_2O_5, with % vanadia loading; the neat titania support being inactive. The limiting electron transfer step seemed to be a function of the catalyst redox properties as well as the induced Lewis acidity. The enhanced activity could thus be attributed to the weakening of V=O bond through the interaction with titania. Superior redox behavior was assumed to arise by presence of labile oxygen atoms in polyvanadate species, rather than the isolated vanadyls [23]. On the other hand, the turnover number, TON, *i.e*., the number of H_2O_2 molecules consumed per unit time per active surface V_2O_5 site, remained almost constant (= 5) with varying the % vanadia, indicating the same rate per each surface V site. Referring to the redox cycles in Scheme **1**, on each V site involved, 5 molecules of H_2O_2 are consumed up to the end of the act. The TON was thus related to the nature of coordination of H_2O_2 to VO_x species, via the various intermediates, rather than to the dispersion mode of vanadia solely.

For co-impregnated samples, of 6 wt % MoO_3 with different wt % vanadia, similar linear increase of the k values with vanadia loading were obtained as shown in Figure **8**(**b**). It is evident that, for co-impregnates and samples of coat 1, (6 Mo–doped x V/T), the rate of limiting step (transformation of X_1 to X_2) had a close trend as in xV/T samples, favoring probably the Mo-V interaction to form surface compound. However, for samples of coat 2, (x V–doped 6 Mo/T), the higher redox activities could be linked with higher dispersion characteristics of the top VO_x species on the surface of titania and/or molybdena. The addition of MoO_3 in different ratios, (3 – 9 wt %), in co-impregnation with 8 wt% vanadia, or addition of 6 wt %, to different x V/T (3 and 5 wt) could lead to a gradual increase in the activity parameter [A] and the turnover number, TON, (Table **1**), referred most probably to competitive interaction behavior of Mo or V on titania surface. The exceptional increase in TON for 9 wt% Mo (=16) in the first series or for 5 wt % V (=19) in the second series could suggest the involvement of multiple surface VO_x and/or MoO_3 sites [6]. This might be evidenced in view of marked decrease in D parameter, with a considerable increase in average particle size (a_e) and some increased relative density of surface patches (α^*_V).

CONCLUSION

In present study, renewed approach was made to optimize the redox functionality of the well-known catalytic system MoO_3-V_2O_5/ TiO_2 (anatase) in relation to various dispersion patterns.

For undoped xV/T samples (of 2-8 wt %), monolayer formation was suggested for x ≥ 8 wt % (9 V/nm^2), below which the degree of dispersion of surface VOx species decreased gradually with % loading. The vanadia phase appeared as growing fused particles with increasing average size and existed as surface patches with increasing density (ranging from easily interacted isolated V^{IV} species to oligomers weakly interacted with TiO_2). The redox activity, expressed in terms of the rate of electron-transfer step in a proposed peroxo intermediates scheme, increased linearly with the vanadia loading. The superior activity was referred to the labile oxygen in the polyvanadate species, rather than to the isolated vanadyls. The constant TON (= 5), indicated the involvement of one surface vanadia site with 5 molecules of H_2O_2 consumed up to the end of the act. It was more related to coordination sequence of H_2O_2 to VO_x species via peroxo intermediates, than to the VOx dispersion mode.

For the samples prepared by co-impregnation of 8 wt % V_2O_5 with different ratios of MoO_3 ranging from 3.0 to 9.0 wt%, the added molybdena could lead to a gradual decrease in dispersion parameters of surface VO_x species. Through competitive interaction of molybdena with titania surface, vanadia particles tended to be aggregated in larger particles, in surface patches with somewhat decreased density, reaching to its maximized effect with 9 wt% Mo. The linear increase of activity parameters in the same profile of xV/T samples could favor the increase of redox characteristics of the sample by Mo presence (through the increase of Lewis acidity), beside the involvement of multiple surface sites of Mo and V. Formation of active non-reducible surface compound via Mo-O-V bridges was suggested. This was confirmed by marked H_2 uptakes with some H-spillover, due to highly stabilized V^{3+} and V^{4+} species. Similar trends were observed in dispersion patterns and reactivity profiles for co-impregnated samples of 6wt% MoO_3 with different x V/T ratios. Specially, with VO_x of 3wt%, some amorphization-like behavior was suggested due to the existence of highly dispersed isolated monomeric species with lower density of surface patches, displayed by competitive linkage of Mo to the surface. In the doped sample of coat 1 (6 Mo–doped 8V/T), the added MoO_3 to VOx species existed in almost monolayer, had the same dispersion and reactivity patterns of the other members of this series, viz., with formation of non-reducible surface compound. The samples of coat 2, (8 V-doped Mo/T), where VOx existed on the top surface of supported MoO_3/TiO_2 in better dispersion state, with higher apparent density of surface patches (α^*_V) exhibiting comparable [A] and TON values to those of xV/T samples. The exceptional increase in TON for 9 wt% Mo and for 5 wt % V (=19) in the co-impregnated series could suggest the involvement of multiple surface VO_x and/or MoO_3 sites, related mainly to the corresponding density of surface patches formed in both cases.

REFERENCES

[1] Fukuan L, Boxiong S, Linghui T, Guoliang L, Chuan H. Powder Technol 2016; 297: 384-391. https://doi.org/10.1016/j.powtec.2016.04.050

[2] Xianming H, Shule Z, Huinan C, Qin Z. J Mol Struct 2015; 1098: 289-297.

[3] Jiahui F, Yanfei Z, Guangda L, Yuanzheng Y. J Non-Cryst Solids 2019; 521: 119491-119496. https://doi.org/10.1016/j.jnoncrysol.2019.119496

[4] Euiseob Y, Jun GL, Dong HK, Yoon SJ, Ja HK, Eun DP, Kwangjin A. J Catal 2018; 368: 134-144.

[5] Yali M, Tuo W, Shuang C, Yujun Z, Xinbin M, Jinlong G. Appl Catal B: Environ 2014; 160: 161-172.

[6] Gheorghita M, Octavian-Dumitru P, Ioan-Cezar M. J Mol Catal A: Chem 2013; 370: 104-110.

[7] Wachs IE, Deo G, Vuurman MA, Hu H, Kim DS, Jehng JM. J Mol Catal 1993: 82, 443-455. https://doi.org/10.1016/0304-5102(93)80046-W

[8] Wachs IE, Deo G, Jehng JM, Kim DS, Hu H, in B.K.Warren and S.T. Oyama (Eds.), "Heterogeneous Hydrocarbon Oxidation", ACS Symp. Ser. 638, American Chemical Society, Washington, DC, 1996, p. 292. https://doi.org/10.1021/bk-1996-0638.ch021

[9] Wachs IE, Saleh RY, Chan SS, Chersich CC. Appl Catal 1985; 15: 339-352. https://doi.org/10.1016/S0166-9834(00)81848-5

[10] Anatasov AI. Chem Eng Proc 2003; 42: 449-460. https://doi.org/10.4324/9780203407899-39

[11] Bulushev DA, Kiwi-Minster L, Zaikovskii VI, Renken A. J Catal 2000; 193: 145-153. https://doi.org/10.1006/jcat.2000.2872

[12] Freitag C, Besselmann S, Loffler E, Grunert W, Rosowski F, Muhler M. Catal Today 2004; 91-92: 143-147. https://doi.org/10.1016/j.cattod.2004.03.023

[13] Corma A, Lopez-Nicto JM, Paredes N, Perez M, Shen Y, Cao H, Suib SL, in", P. Ruiz, B. Delmon (Eds.), "New Developments in Selective Oxidation by Heterogeneous Catalysis", Elsevier Science Publ., Stud Surf Sci Catal 1992; 72: 213. https://doi.org/10.1016/S0167-2991(08)61673-0

[14] Routray K, Reddy KRSK, Deo G. Appl Catal A: Gen 2004; 265: 103-113. https://doi.org/10.1016/j.apcata.2004.01.006

[15] Wong WC, Nobe K. Ind Eng Chem Prod Res Dev 1984; 23: 564-568. https://doi.org/10.1021/i300016a010

[16] Hyoung-Lim K, Hea-Kyung P. J Ind Eng Chem 2013; 19: 73-79.

[17] Camposeco R, Castillo S, Mugica V, Mejia-Centeno I, Marín J. Catal Commun 2014; 45: 54-58. https://doi.org/10.1016/j.catcom.2013.10.025

[18] Schraml-Marth M, Wokaun A. J Chem Soc Faraday Trans 1991; 87: 2635-2646. https://doi.org/10.1039/ft9918702635

[19] Roman B, Pavel Č, Michal S. Physics Procedia 2013; 44: 195-205. https://doi.org/10.1016/j.phpro.2013.04.024

[20] Deo G, Watchs IE, Haber J. Crit Rev Surf Chem 1994; 4: 141-150.

[21] Xuwen C, Bing Y, Patryk O, Yanzheng G, Xinjie Y, Wanting L, Michael GW. Chem Eng J 2019; 364: 79-88.

[22] Nedyalkova R, Ilieva L, Bernard MC, Hugot-Le GA, Andreeva D. Mater Chem Phys 2009; 116: 214-218. https://doi.org/10.1016/j.matchemphys.2009.03.012

[23] Renata TS, Małgorzata W, Robert G. Catal Today 2005; 99: 241 253. https://doi.org/10.1016/j.cattod.2004.09.046

[24] Kornelak P, Borzecka-Prokop B, Litynska-Dobrzynska L, Wagner J, Su DS, Camra J, Wesełucha-Birczynska A. Catal Today 2007; 119: 204-208. https://doi.org/10.1016/j.cattod.2006.08.042

[25] Huang X, Peng Y, Liu X, Kezhi L, Deng Y, Li J. Catal Commun 2015; 69: 161-164. https://doi.org/10.1016/j.catcom.2015.04.020

[26] Chary KVR, Bhaskar T, Seela KK, Lakshmi KS, Reddy KR. Appl Catal A: Gen 2001; 208: 291-305. https://doi.org/10.1016/S0926-860X(00)00724-9

[27] Chary KVR, Reddy KR, Kumar CP, Catal Commun 2001; 2: 277-284. https://doi.org/10.1016/S1566-7367(01)00044-9

[28] Sigel H and Sigel A (Eds.), "Metal Ions in Biological Systems, Vanadium and its Role in Life", Vol. 31, Marcel Dekker, New York (1995).

[29] Barbara F, Federica S, Alessia C, Valeria C. Catal Today 2017; 285: 49-56.

[30] Kioseoglou E, Petanidis S, Gabriel C, Salifoglou A. Coord Chem Rev 2015; 301-302: 87-105. https://doi.org/10.1016/j.ccr.2015.03.010

[31] Islam NS, Boruah JJY. J Chem Sci 2015; 127: 777-795. https://doi.org/10.1007/s12039-015-0833-y

[32] Gekhman AE, Amelichkina GE, Moiseeva NI, Vargaftik MN, Moiseev I I. J Mol Catal 2000; 162: 111-124. https://doi.org/10.1016/S1381-1169(00)00325-3

[33] Virgílio JM, Ferreira N, Thiago DSBC, André LLM, Alexandre BG, Paulo GPDO, Fabiana MTM. Mol Catal 2018; 458: 317-325.

[34] Zhang J, Yang H, Sun T, Chen Z, Yin G. Inorg Chem 2017; 56: 834-844. https://doi.org/10.1021/acs.inorgchem.6b02277

[35] Shimoyama Y, Kojima T. Inorg Chem 2019; 58: 3676-3682. https://doi.org/10.1021/acs.inorgchem.8b03245

[36] Hassan SA, Mekewi MA, Shebl FA, Sadek SA. J Materials Sci 1991; 26: 3712-3720. https://doi.org/10.1007/BF01184961

[37] Roozeboom F, Fransen T, Mars P, Gellings PJ, Anorg Z. Allg Chem 1997; 449: 25-40. https://doi.org/10.1002/zaac.19794490102

[38] Roiter VA, "Catalytic Properties of Materials", Handbook-(Naukova Dumka), Academy of Science, Institute of Physical Chemistry, Kiev, Ukraniya 1968; pp. 539 and 721.

[39] Joint Committee on Powder Diffraction Standards, JCPDS, (1971) file no. 9-387.

[40] Lietti L, Nova I, Ramis G, Dall'Acqua L, Busca G, Giamello E, Forzatti P, Bregani F. J Catal; 1999; 187: 419-435 https://doi.org/10.1006/jcat.1999.2603

[41] Xiong LB, Li JL, Yang B, Yu Y. J Nanomater 2012; Article ID 831524: 1-13. https://doi.org/10.1155/2012/831524

[42] Busca G, Centi G, Marchetti L, Triffiro F., Langmuir; 1986: 2(5): 568-577. https://doi.org/10.1021/la00071a007

[43] Catana AG, Rao RR, Weckhuysen BM, Van Der Voort P, Vansant E, Schoonheydt R. J Phys Chem B 1998; 102: 8005-8012. https://doi.org/10.1021/jp981482s

[44] Balikdjian JP, Davidson A, Launay S, Eckert H, Che M. J Phys Chem B 2000; 104: 8931-8939. https://doi.org/10.1021/jp000569m

[45] Vedrine JC, Catal Today 2000; 56: 455-460. https://doi.org/10.1016/S0040-4020(99)01014-5

[46] Qi C, Bao W, Wang L, Li H, Wu W. Catal 2017; 7: 110-123. https://doi.org/10.3390/catal7040110

[47] Gannoun C, Delaigle R, Ghorbel A, Gaigneaux EM. Catal Sci Technol 2019; 9: 2344-2350. https://doi.org/10.1039/C9CY00099B

[48] Mei C, Li L, Mei D, Zhao X, Zhao X, Yuan Y. Res Environ Sci 2016; 29: 1665-1671.

[49] Gobara HM, Hassan SA. Petrol Sci Technol 2009; 27: 1555-1571. https://doi.org/10.1080/10916460802608677

Received on 22-09-2019 Accepted on 13-11-2019 Published on 21-11-2019

http://dx.doi.org/10.15379/2408-9834.2019.06.02.01